Supplementary Information (SI) for Green Chemistry.
This journal is © The Royal Society of Chemistry 2026

Supplementary Information

Domino Photoreduction of CO_2 to CH_4/C_2H_6 by Steering Catalyst Amounts

Minzhi Ma[a, b]*, Mengge Jia[a], Shichu Zhao[a, c], Zhiqiang Jiang[d], Kangle Lv[d], Tongqing Li[a], Helei Chai[a], Yan Lei[a], Jingjing Si[a], Zhi Zheng[a], Wenjun Fa[a, c]*

[a] Key Laboratory of Micro-Nano Materials for Energy Storage and Conversion of Henan Province, Institute of Surface Micro and Nano Materials, College of Chemical and Materials Engineering, Xuchang University, Xuchang, Henan 461000, China

[b] Key Lab for Special Functional Materials, Ministry of Education, National & Local Joint Engineering Research Center for High-Efficiency Display and Lighting Technology, School of Materials Science and Engineering, Collaborative Innovation Center of Nano Functional Materials and Applications, Henan University, Kaifeng, 475004, China

[c] School of Materials Science and Engineering, Zhengzhou University, Zhengzhou, Henan 450001, China

[d] Key Laboratory of Catalysis and Energy Materials Chemistry of Ministry of Education, College of Resources and Environment, South-Central Minzu University, Wuhan, 430074, China

* Corresponding authors: Minzhi Ma (Minzhima@yeah.net), Wenjun Fa (fa_wenjun@163.com)

Table of contents

1.1 Photocatalytic reaction device

Figure S1. Photocatalytic reduction of the CO_2 reaction system.

1.2 Technical details of the reactor

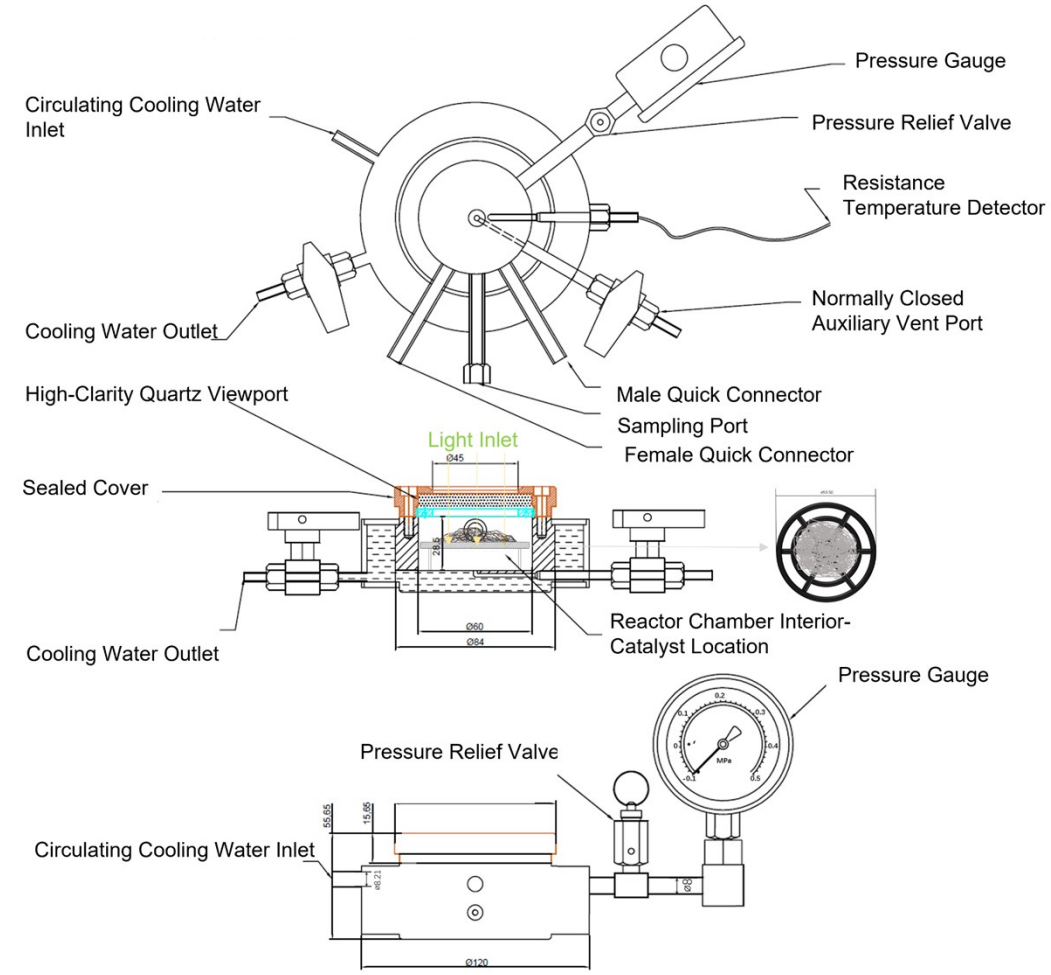

Chamber material: SUS304 (AISI 304) stainless steel. All pipes not otherwise specified have a diameter of 6 mm.

Figure S2. Design drawing of the photocatalytic reaction apparatus.

1.3 Mixing effect diagram of quartz cotton and catalyst

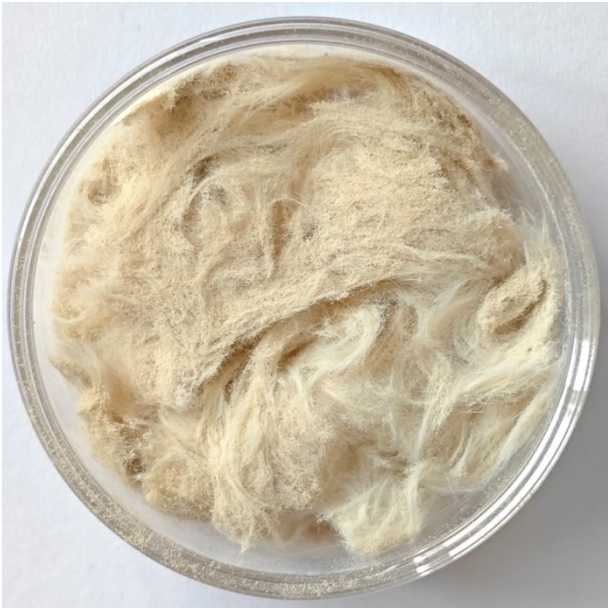

Figure S3. Mix 200 mg of quartz cotton with 200 mg of Ni/CeO_2.

1.4 Internal gas circuit diagram of gas chromatography

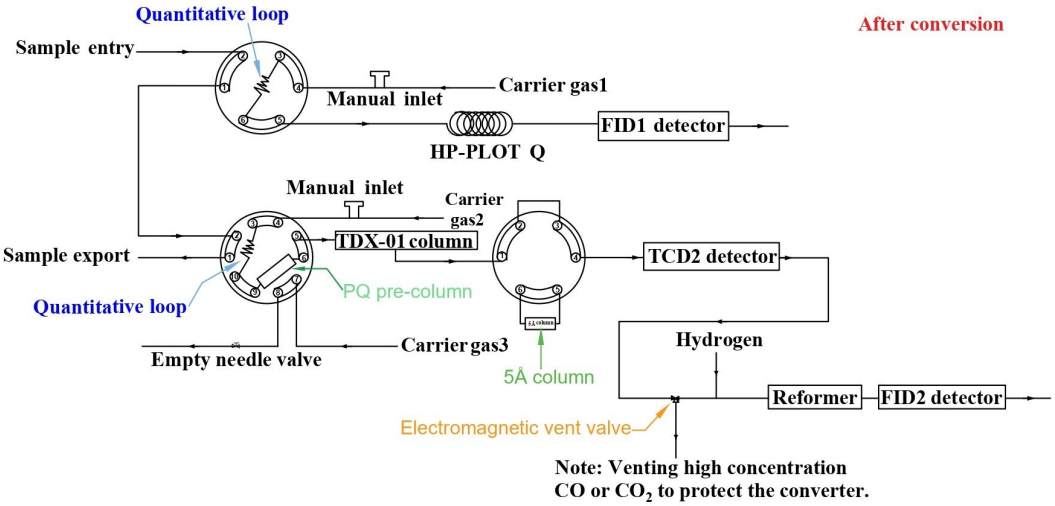

Figure 4. Schematic diagram of internal gas flow path of gas chromatography.

1.5 Gas chromatography (GC) curves

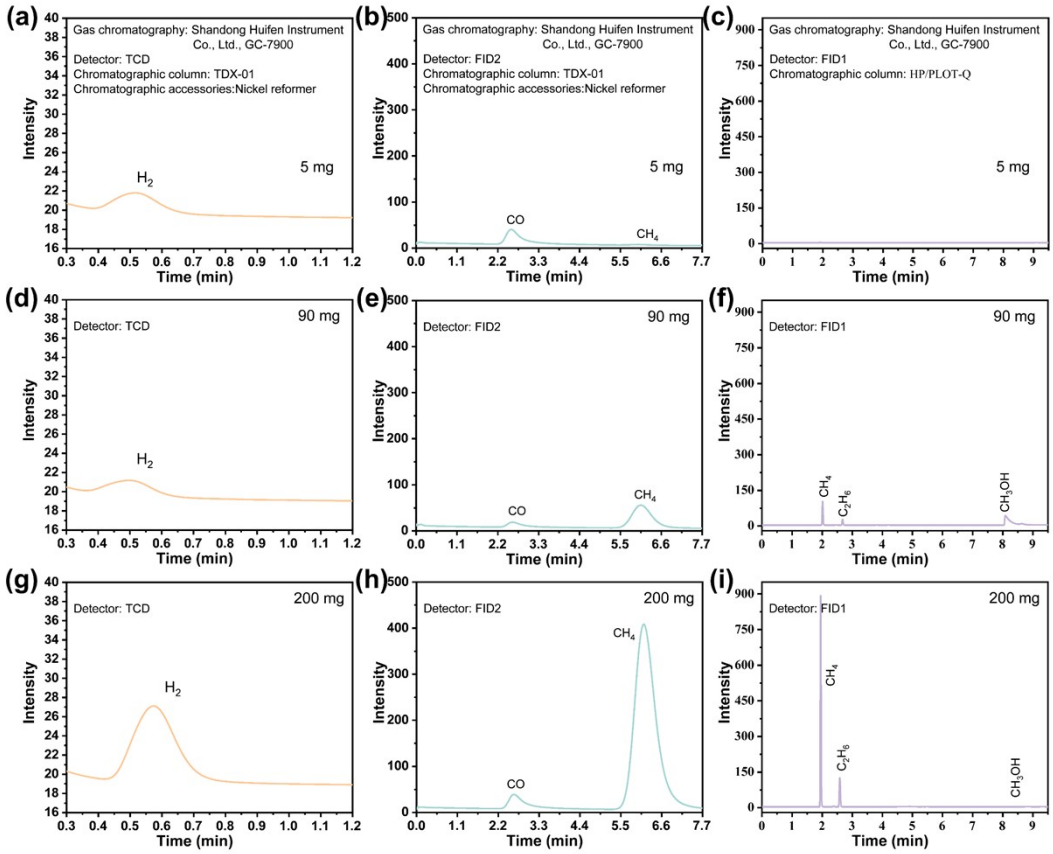

Figure S5. Results of GC analysis in the photoreduction of CO_2 reaction for the Ni/CeO_2 with different amount after light irradiation 4 h. 5 mg of (a) TCD, (b) FID2, (c) FID1; 90 mg of (d) TCD, (e) FID2, (f) FID1; 200 mg of (g) TCD, (h) FID2, (i) FID1.

1.6 The calibration curves

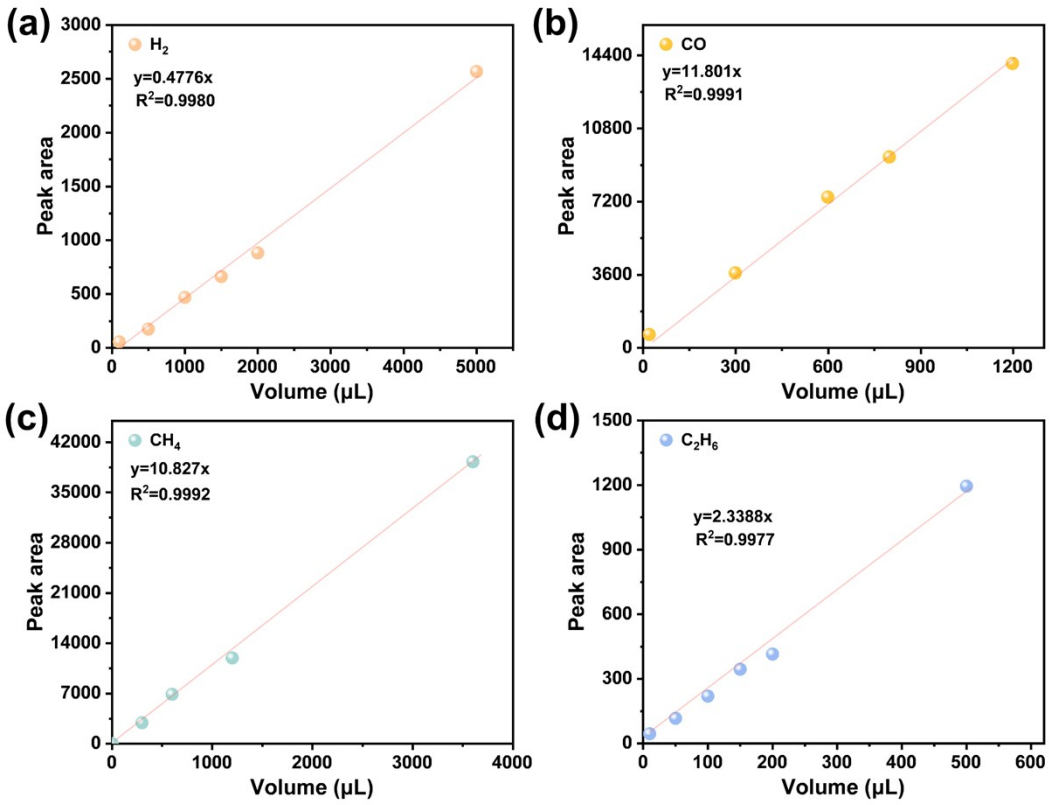

Figure S6. Calibration curves of CO_2 photoreduction products. (a) H_2; (b) CO; (d) CH_4; (e) C_2H_6.

The detailed procedure for calibration is as follows. The yield of products in the reactor was calibrated using the external standard method. The H_2, CO, CH_4, and C_2H_6 used for calibration were all high-purity standard gases (99.99%). A certain amount of the aforementioned four gases was injected into the reactor, which was at room temperature (30 °C) and atmospheric pressure. The exact volume used for each calibration gas is shown in **Figure S6**. A gas mixture of 20% CO_2 in Ar served as the balance gas. Of note, to ensure the consistency between the calibration and testing conditions as much as possible, the calibration gases were used as a mixture for simultaneous calibration, rather than calibrating each gas individually. Subsequently, the temperature and pressure of the reactor were adjusted to be consistent with those used in the standard activity tests. After collecting three data points from the reactor, we cooled and depressurized the system, after which the reactor was opened and cleaned. Finally, the entire procedure described above was repeated three to four times. The mean was calculated from the entire dataset following the exclusion of outliers. The net volume of the reactor was determined to be 80.5 mL by water displacement. The reaction pressure during testing at 180 °C was approximately 0.4 MPa. Additionally, the pressure change in the reactor before and after sampling was extremely slight. Gas samples were withdrawn from the reactor using a gas-tight syringe under controlled conditions (the sampling syringe was maintained at 30 °C and atmospheric pressure). Through the above procedure, the expression for the correspondence between gas products (volume) and GC peak area can be obtained (**Figure S6**). From the known GC peak areas, the product yields (volume) were determined. The amount of each specific product (in moles) was then calculated using the ideal gas law ($PV=nRT$).

1.7 UV-vis spectra of the mixtures with different catalysts and quartz wool

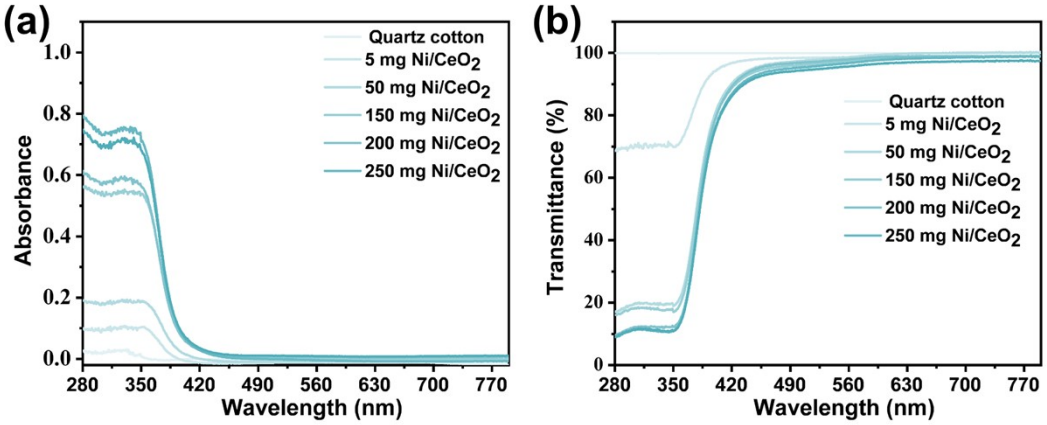

Figure S7. UV-vis diffuse reflectance spectra of the catalyst (Ni/CeO_2) mixed with quartz wool at different loadings. (a) UV-vis absorption spectra of the mixed catalyst/quartz wool samples; (b) UV-vis transmission spectra of the mixed catalyst/quartz wool samples.

1.8 Yield of CO and H_2 at 180 °C

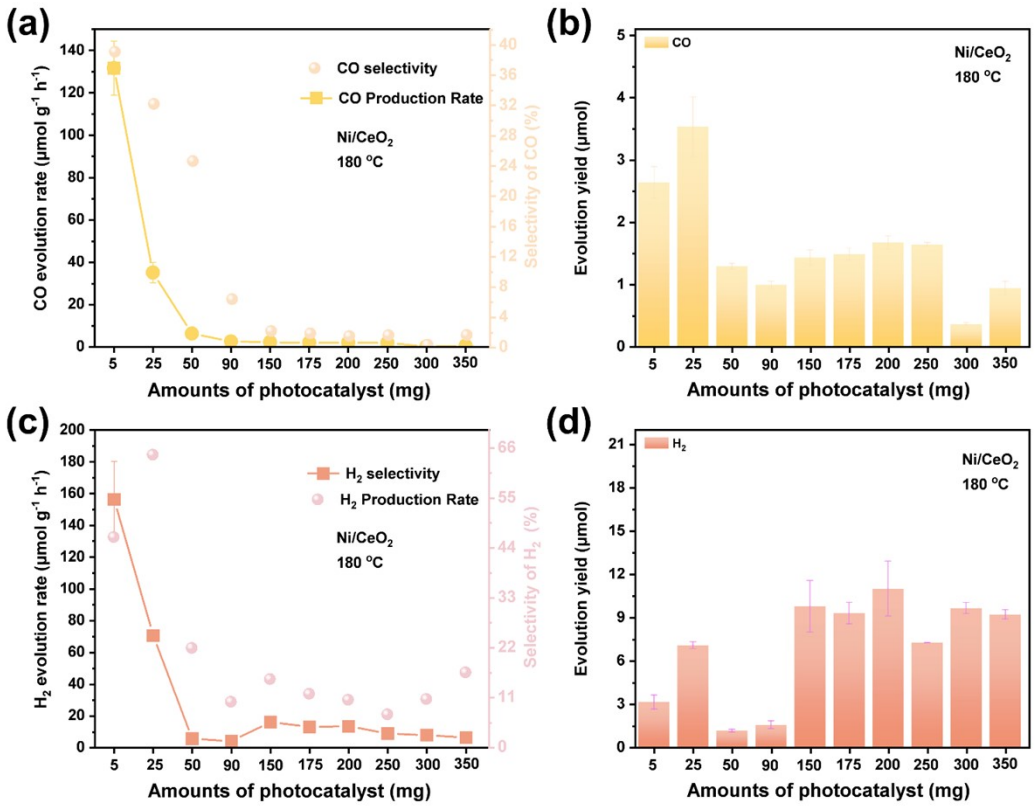

Figure S8. Photocatalytic CO_2 reduction performance under light irradiation for 4 h at 180 °C over Ni/CeO_2. (a) CO evolution rates and selectivities; (b) CO yield; (c) H_2 evolution rates and selectivities; (b) H_2 yield.

1.9 Yield of CO and H_2 at 80 °C

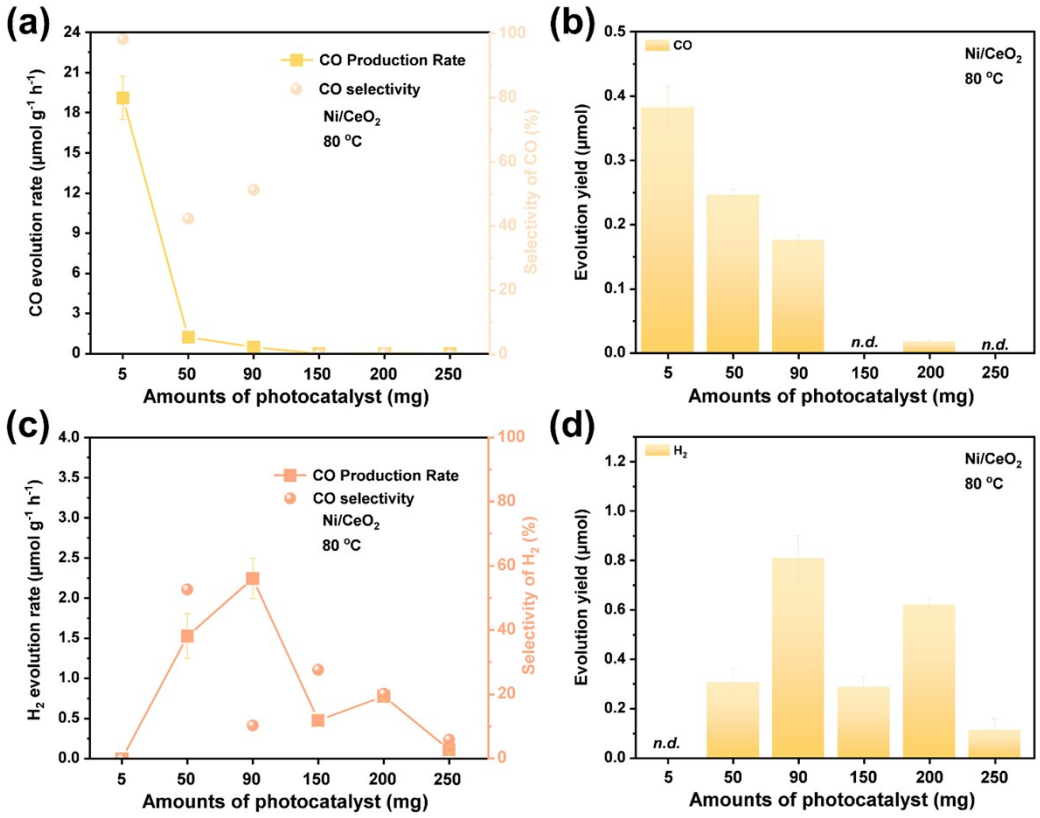

Figure S9. Photocatalytic CO_2 reduction performance under light irradiation for 4 h at 80 °C over Ni/CeO_2. (a) CO evolution rates and selectivities; (b) CO yield; (c) H_2 evolution rates and selectivities; (b) H_2 yield.

1.10 Dependence of product selectivity on catalyst amount at 25 °C

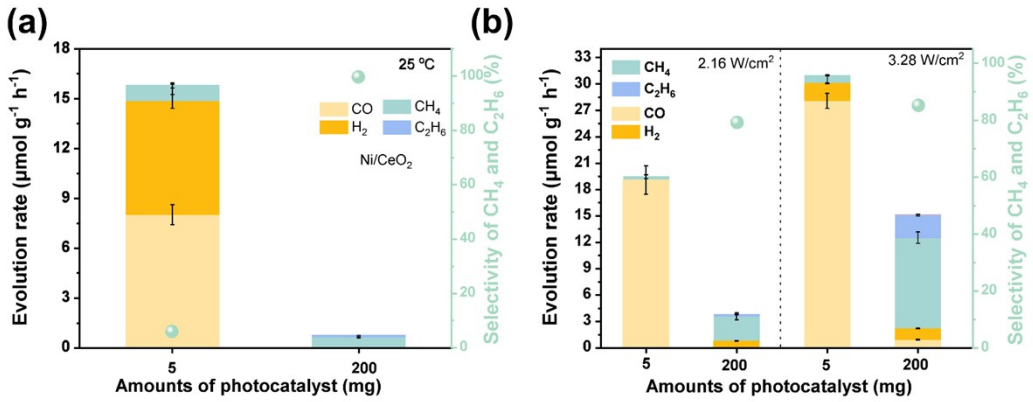

Figure S10. Photocatalytic CO_2 reduction performance under light irradiation for 4 h over Ni/CeO_2. (a) at 25 °C; (b) at different light intensities at 80 °C.

1.11 Yield of CO_2 reduction products over 4 hours

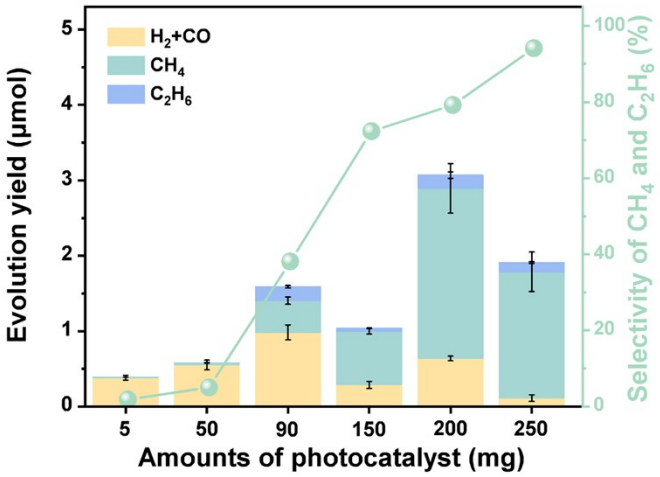

Figure S11. Photocatalytic CO_2 reduction performance under light irradiation for 4 h at 80 °C over Ni/CeO_2.

1.12 XRD patterns of the reference samples

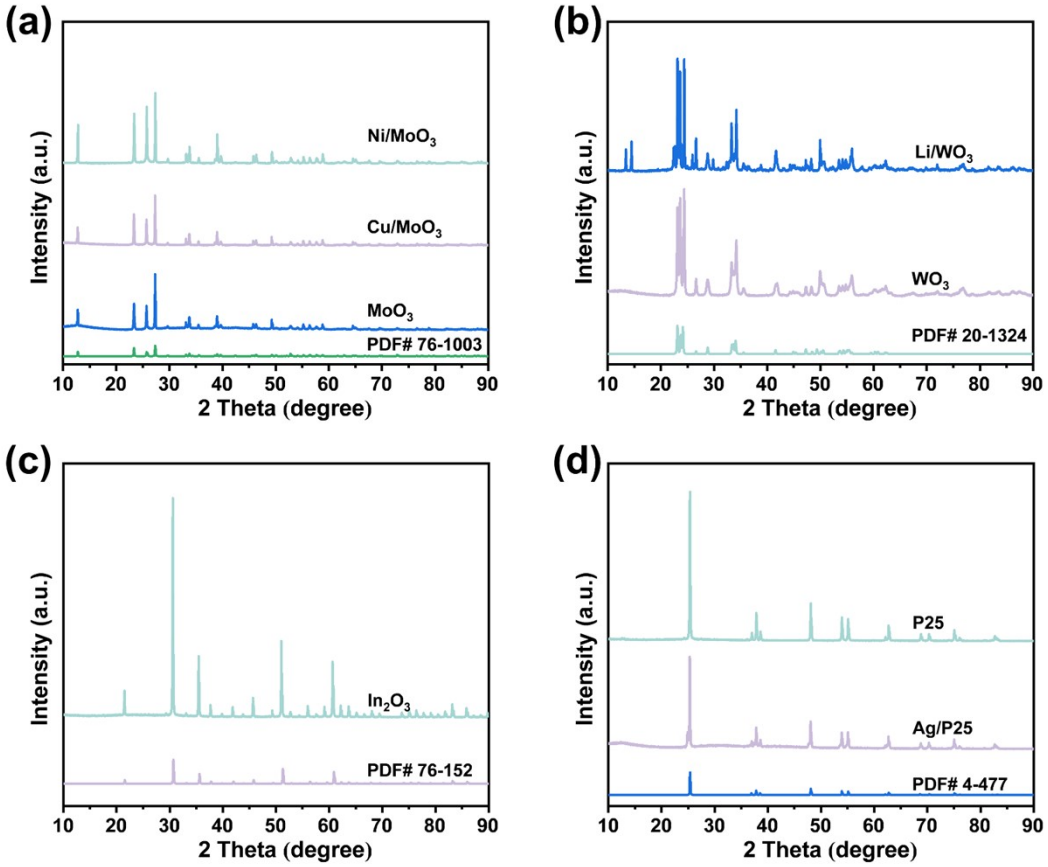

Figure 12. XRD pattern of the sample. (a) MoO_3, Cu/MoO_3, Ni/MoO_3; (b) Li/WO_3, WO_3; (c) In_2O_3; (d) P25, Ag/P25.

1.13 SEM images and elemental mapping

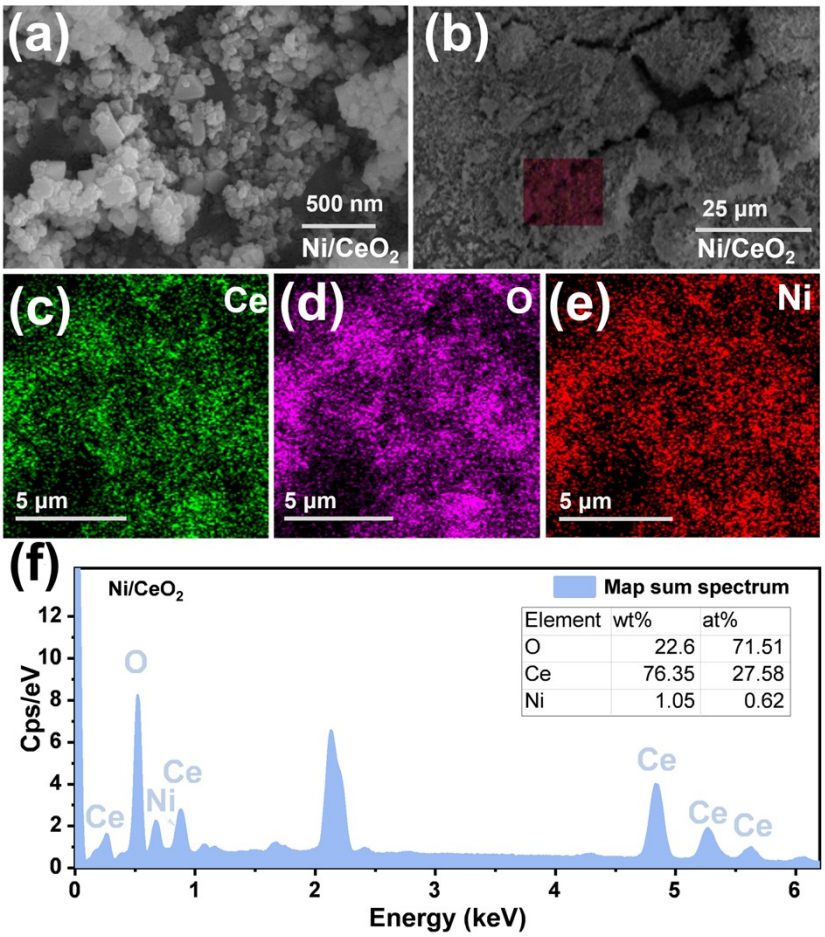

Figure S13. SEM images (a–b) and corresponding elemental mapping of (c) Ce, (d) O, (e) Ni, (f) map sum spectrum over the Ni/CeO_2.

1.14 XPS patterns of Ni/CeO_2

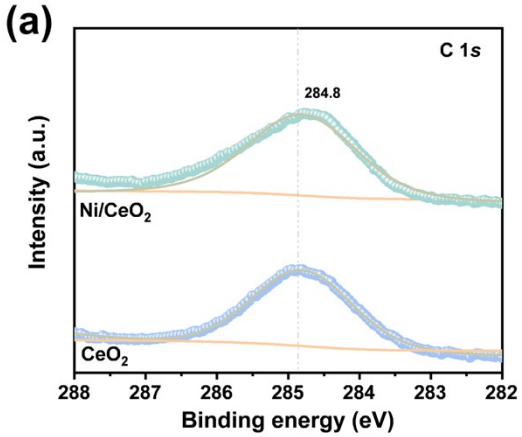

Figure S14. High-resolution XPS spectra of C 1*s*.

1.15 Electronic structure of the as-prepared catalysts

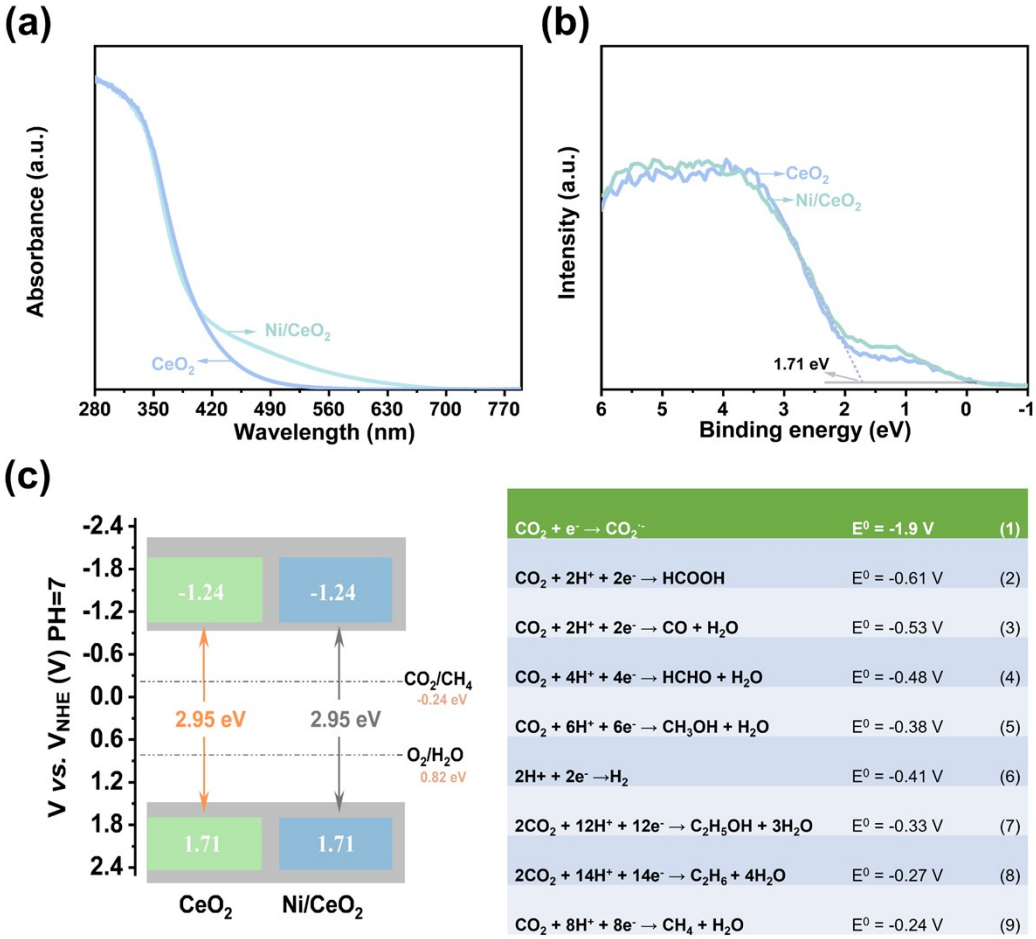

Figure S15. Band structure of CeO_2 and Ni/CeO_2. (a) UV-vis spectra; (b) XPS valance spectra; (c) Band structure.

1.16 High-resolution XPS spectra in light

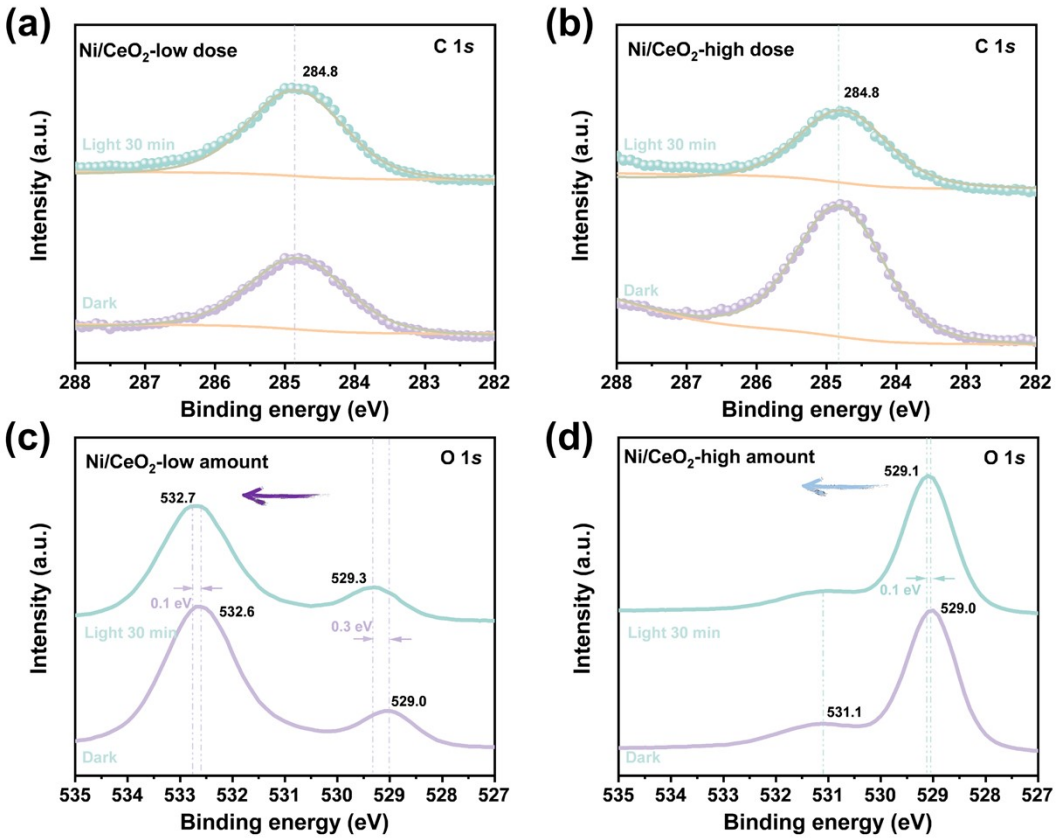

Figure S16. High-resolution XPS spectra in light. The C 1*s* spectra of the Ni/CeO_2-low amount (a) and the Ni/CeO_2-high amount (b); The O 1*s* spectra of the Ni/CeO_2-low amount (c) and the Ni/CeO_2-high amount (d).

1.17 *In situ* DRIFTS spectra of Ni/CeO_2 for CO adsorption

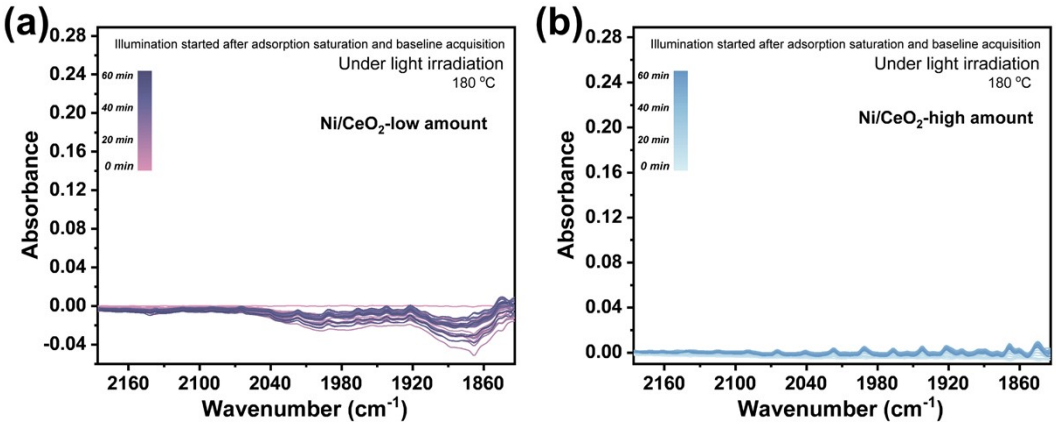

Figure S17. *In situ* DRIFTS spectra for CO adsorption under light irradiation during photocatalytic CO_2 reduction with H_2O. (a) Low Ni/CeO_2 catalyst amount; (b) high Ni/CeO_2 catalyst amount.

1.18 Compared with the reported work

Table S1. Comparison of CO_2-to-CH_4 photocatalysis with H_2O over the past five years.

Photocatalyst	Light source	Reaction feedstock	CH_4 evolution rate ($\mu mol \cdot h^{-1}$)	CH_4 sel.	Refs.
Ni/CeO_2	300 W Xe lamp	200 mg catalysts 0.04 MPa CO_2 and 1 mL H_2O	20.7979	83.28%	This work
Rb:CABB	300 W Xe lamp	5 mg catalysts CO_2 and 100 μL H_2O	0.0145	48.60%	[1]
WO_3/In_2O_3	300 W Xe lamp	50 mg catalysts 70 kPa CO_2 and 1 mL H_2O	0.0225	45%	[2]
CuO/NUS-8	300 W Xe lamp	3 mg catalysts 50 kPa CO_2 and 1 mL H_2O	0.0489	81.43%	[3]
Cu-ZnTCPP/g-C_3N_4	300 W Xe lamp	5 mg catalysts 10% CO_2、20% O_2、70% Ar and H_2O	0.0565	35%	[4]
Ni_{SA}-NiO_x/TiO_2	300 W Xe lamp	5 mg catalysts CO_2 and 1 mL H_2O	0.0778	87.60%	[5]
Mg:CdS QDs	300 W Xe lamp	2 mg catalysts CO_2 and 4 mL H_2O、1 mL TEOA	0.0916	88.70%	[6]
Nb−$W_{18}O_{49}$	300 W Xe lamp	5 mg catalysts 0.1 MPa CO_2 and 1 mL H_2O	0.1014	82.60%	[7]
$Pd/Cu_3(HITP)_2/TiO_2$	300 W Xe lamp	5 mg catalysts CO_2 and 5 mL H_2O	0.1495	~100%	[8]
60ISIO-3h	300 W Xe lamp	10 mg catalysts CO_2 and H_2O	0.1652	95.93%	[9]
PDA/Pd_{SA}/TiO_2	300 W Xe lamp	5 mg catalysts CO_2 (99.999%) and 100 μL H_2O	0.1864	98.13%	[10]
TiO_2-V_i	300 W Xe lamp	10 mg catalysts 101 kPa CO_2 and 1 mL H_2O	0.194	~100%	[11]
PW_9/g-C_3N_4	300 W Xe lamp	5 mg catalysts CO_2 (99.99%) and 100 μL H_2O	0.204	80%	[12]
Ag/TiO_2	300 W Xe lamp	5 mg catalysts CO_2 and 200 μL H_2O	0.23	71.43%	[13]
Co_1In_1/CN	300 W Xe lamp	20 mg catalysts CO_2 and 1 mL H_2O	0.376	79%	[14]
$ZnCoO_x$/N-GC	300 W Xe lamp	50 mg catalysts CO_2 and H_2O	0.38	61.30%	[15]
Co-BS	300 W Xe lamp	25 mg catalysts CO_2 and 1 mL H_2O	0.39	58.60%	[16]
Ru-O_V/TiO_2	300 W Xe lamp	10 mg catalysts CO_2 (99.99%) and 500 μL H_2O	0.501	81.00%	[17]
Cu-SA-CO	300 W Xe lamp	10 mg catalysts 0.2 MPa CO_2 and 0.3 mL H_2O	0.585	~100%	[18]
Bi/TiO_2	300 W Xe lamp	10 mg catalysts CO_2 and 200 μL H_2O	0.6023	62.11%	[19]
S-Ti_3C_2	300 W Xe lamp	10 mg catalysts CO_2 and 10 mL H_2O	0.6517	94.05%	[20]
CZ_v1S	300 W Xe lamp	5 mg catalysts 70 kPa CO_2 and 10 mL H_2O	0.6675	85.40%	[21]
Cu_2O@NH_2-CuBTC	300 W Xe lamp	10 mg catalysts 80 kPa CO_2 and 2 mL H_2O	0.708	98.60%	[22]
Au/TiO_2-V_{Ti}	300 W Xe lamp	5 mg catalysts CO_2 and 5 mL H_2O	0.7825	~100%	[23]
A-V_o-SnO_2	300 W Xe lamp	50 mg catalysts 100 kPa CO_2 and 0.2 mL H_2O	0.8635	93.80%	[24]
Bi_2S_3-SnS_2	300 W Xe lamp	5 mg catalysts CO_2 and 2 mL H_2O	1.707	94.60%	[25]
hS-ZnSe/CdSe	300 W Xe lamp	10 mg catalysts CO_2 and 30 mL CH_3CN、10 mL H_2O、10 mL TEOA	2.155	92%	[26]
Zn/GaN NWs/Si	300 W Xe lamp	0.0136 mg catalysts CO_2 and 5 mL H_2O	2.57	93.60%	[27]
Pd/ZnO-V_o	300 W Xe lamp	10 mg catalysts CO_2 and 5 mL H_2O	2.576	95.30%	[28]
Sn-BMO	300 W Xe lamp	20 mg catalysts CO_2 (99.999%) and 2 mL H_2O	4.146	95.70%	[29]

1.19 References

[1] Z. Chen, X. Jiang, H. Xu, J. Wang, M. Zhang, D. Pan, G. Jiang, M. Z. Shahid and Z. Li, Small, **2024**, 20, 2401202.

[2] Y. He, Z. Yang, J. Yu, D. Xu, C. Liu, Y. Pan, W. Macyk and F. Xu, Journal of Materials Chemistry A, **2023**, 11, 14860-14869.

[3] X. Huang, Z. Wang, Y. Jiang, W. Wen, S. Chen, X. Han, J. Chen, S. Deng and J. Wang, Chemical Engineering Journal, **2026**, 527, 171767.

[4] S. Xie, C. Deng, Q. Huang, C. Zhang, C. Chen, J. Zhao and H. Sheng, Angewandte Chemie International Edition, **2023**, 62, e202216717.

[5] S. Wei, Y. Li, M. Xu, T. Wang, Y. Tu and B. Li, Journal of Colloid and Interface Science, **2024**, 683, 731-741.

[6] J. Liu, Z. Liu, P. Lu, J. Wang, Y. Lu, S. Xu, G. Jiang, S. Li, J. Shao and Z. Li, Advanced Functional Materials, **2025**, 36, e09666.

[7] S. Wei, Y. Li, M. Xu, W. Hu and B. Li, ACS Applied Materials & Interfaces, **2025**, 17, 33975-33986.

[8] W.-h. Bai, Q. Shao, Y.-k. Ji, H. Dong, X.-y. Hu, H.-r. Xiao and C. Long, Angewandte Chemie International Edition, **2025**, 64, e202513157.

[9] K. Lai, Y. Sun, N. Li, Y. Gao, H. Li, L. Ge and T. Ma, Advanced Functional Materials, **2024**, 34, 2409031.

[10] Z. A. Zhao, C. Zhang, J. Shen, C. Gao, Q. Cai, J. Jiang, C. Fu, X. Xu, W. Dai and Z. Zhang, Advanced Functional Materials, **2025**, e22529.

[11] Y. He, S. Dai, J. Sheng, Q. Ren, Y. Lv, Y. Sun and F. Dong, Proceedings of the National Academy of Sciences, **2024**, 121, e2322107121.

[12] Q. Zhu, Z. Li, T. Zheng, X. Zheng, S. Liu, S. Gao, X. Fu, X. Su, Y. Zhu, Y. Zhang and Y. Wei, Angewandte Chemie International Edition, **2025**, 64, e202413594.

[13] C. Ban, Y. Wang, Y. Feng, Z. Zhu, Y. Duan, J. Ma, X. Zhang, X. Liu, K. Zhou, H. Zou, D. Yu, X. Tao, L. Gan, G. Han and X. Zhou, Energy & Environmental Science, **2024**, 17, 518-530.

[14] B. Hu, Z. Li, B. Wang, L. Chen, X. Wang, X. Hu, Z. Bai, Y. Li, G. Chen, X. Luo and S.-F. Yin, Applied Catalysis B: Environment and Energy, **2025**, 371, 125196.

[15] X. Bai, L. He, W. Zhang, T. Yang, F. Lv, Y. Xiong, Z. Zhang and Y. Zhao, Chemical Engineering Journal, **2025**, 509, 161312.

[16] S. She, L. Chen, K. Liao, Y. Fu, J. Wang and X. Wu, Journal of Colloid and Interface Science, **2024**, 663, 947-960.

[17] C. Feng, M. Hu, S. Zuo, J. Luo, P. Castaño, Y. Ren, M. Rueping and H. Zhang, Advanced Materials, **2025**, 37, 2411813.

[18] W. Zhang, C. Deng, W. Wang, H. Sheng and J. Zhao, Advanced Materials, **2024**, 36, 2405825.

[19] J. Meng, K. Wang, Y. Wang, J. Ma, C. Ban, Y. Feng, B. Zhang, K. Zhou, L. Gan, G. Han, D. Yu and X. Zhou, Nano Research, **2023**, 17, 1190-1198.

[20] Y. Chen, X. Lin, W. Li, H. Sun, S. Jia, Y. Zhou, Y. Hao, Z. Liu, S. Yin, C. Guo, Y. Sun, P. Huo, C. Li, Y. H. Ng, J. Crittenden, Z. Zhu and Y. Yan, Advanced Functional Materials, **2024**, 34, 2400121.

[21] Y. Wang, Z. Zhou, Y. Xu, R. Zhao, R. Feng, P. Yu and Y. Liu, Advanced Functional Materials, **2025**, 35, 2504435.

[22] Z. Tang, Y. Wang, J. Xiong, X. Wang, X. Li, J. Wang, Y. Liu, Z. Zhao and Y. Wei, Applied Catalysis B: Environment and Energy, **2025**, 381, 125872.

[23] K. Zheng, B. Li, Y. Zheng, X. Zhang, R. Chen, S. Zhang, S. Liu, J. Zhu, J. Liu, W. Liu, J. Hu, C. Liu, F. Sun, Z. Dai, Y. Sun and Y. Xie, Advanced Energy Materials, **2026**, e06793.

[24] Y. Huo, P. Zhang, J. Chi, F. Fang, Y. Song and D. Sun, Advanced Energy Materials, **2024**, 14, 2304282.

[25] M. Wu, X. Wang, Y. Zheng, P. Lan, A. Hu, J. Zhu, B. Li, Y. Wu, J. Hu, C. Liu, J. Zhu, Y. Pan, M. Zhou, Y. Sun and Y. Xie, Journal of the American Chemical Society, **2025**, 147, 45660-45669.

[26] X. Gao, Z. Zhao, Z. Wu, Z. Yang, K. Guo, J. Han, Y.-H. Ra, X. Kong, J. Zhu and Y. Wang, Advanced Materials, **2025**, 38, e14658.

[27] M. S. Nasir, B. Sheng, Y. Zhao, H. Ye, J. Song, J. Li, P. Wang, T. Wang, X. Wang, Z. Huang and B. Zhou, Science Bulletin, **2025**, 70, 373-382.

[28] K. Zheng, S. Liu, J. Zhu, Z. Dai, C. Liu, B. Li, Y. Zheng, X. Chen, L. Zhai, Y. Wu, W. Liu, M. Fan, J. Hu, Y. Pan, J. Zhu, F. Sun, Y. Sun and Y. Xie, Angewandte Chemie International Edition, **2025**, 64, e202508259.

[29] Q. Liang, J. Fan, X. Deng, J. Liu, J. Zeng, H. Zhang, J. Li, C. Liu, Z. Kang and Z. Zhao, Angewandte Chemie International Edition, **2025**, 65, e21874.